



# The inverse problem in electroencephalography using the bidomain model of electrical activity

Alejandro Lopez Rincon\*, Shingo Shimoda

RIKEN BSI-TOYOTA Collaboration Center, 2271-130 Anagahora, Shimoshidami, Moriyama-ku, Nagoya, Aichi 463-0003, Japan

## HIGHLIGHTS

- The EEG inverse problem is solved using the bidomain model.
- A spatial comparison is made with fMRI using the linkRBrain platform.
- Accuracy is increased in comparison with other methods (MNE and LORETA).

## ARTICLE INFO

### Article history:

Received 17 May 2016

Received in revised form

28 September 2016

Accepted 28 September 2016

Available online 11 October 2016

### Keywords:

EEG

Bidomain

Regularization

Inverse problem

## ABSTRACT

**Background:** Acquiring information about the distribution of electrical sources in the brain from electroencephalography (EEG) data remains a significant challenge. An accurate solution would provide an understanding of the inner mechanisms of the electrical activity in the brain and information about damaged tissue.

**New Method:** In this paper, we present a methodology for reconstructing brain electrical activity from EEG data by using the bidomain formulation. The bidomain model considers continuous active neural tissue coupled with a nonlinear cell model. Using this technique, we aim to find the brain sources that give rise to the scalp potential recorded by EEG measurements taking into account a non-static reconstruction.

**Comparison with Existing Methods:** We simulate electrical sources in the brain volume and compare the reconstruction to the minimum norm estimates (MNEs) and low resolution electrical tomography (LORETA) results. Then, with the EEG dataset from the EEG Motor Movement/Imagery Database of the Physiobank, we identify the reaction to visual stimuli by calculating the time between stimulus presentation and the spike in electrical activity. Finally, we compare the activation in the brain with the registered activation using the LinkRbrain platform.

**Results/Conclusion:** Our methodology shows an improved reconstruction of the electrical activity and source localization in comparison with MNE and LORETA. For the Motor Movement/Imagery Database, the reconstruction is consistent with the expected position and time delay generated by the stimuli. Thus, this methodology is a suitable option for continuously reconstructing brain potentials.

© 2016 The Author(s). Published by Elsevier B.V. This is an open access article under the CC BY license (<http://creativecommons.org/licenses/by/4.0/>).

## 1. Introduction

Neural processes are generated by the propagation of electrical activity in the brain. This activity produces electrical potentials that can be measured through electrodes in various positions on the scalp, a technique referred to as electroencephalography (EEG). This voltage distribution on the scalp is generated from the extracellular current by the post-synaptic potentials in the apical dendrites of pyramidal neurons inside the brain. EEG signals, in comparison

with other brain imaging techniques, have the advantage of high temporal resolution, but they have a small amplitude (on the order of hundred of  $\mu$ V) and are highly susceptible to noise.

The electrical activity of the brain is described by the volume conductor model with current sources using Poisson's equation coupled with Neumann and Dirichlet boundary conditions (Hallez et al., 2007a). Simulating the potentials at the electrode positions from current sources inside the brain is known as the EEG forward problem; inference of the position of the current sources from electrode potentials is known as the EEG inverse problem or the neural source imaging problem (Grech et al., 2008; Brannon et al., 2008).

The EEG inverse problem is fundamental in neuroscience, as it gives insight about spatial and temporal activity in the brain for different tasks. An accurate solution of the neural source imaging

\* Corresponding author.

E-mail addresses: [alejandro.lopezrn@hotmail.com](mailto:alejandro.lopezrn@hotmail.com) (A. Lopez Rincon), [shimoda@brain.riken.jp](mailto:shimoda@brain.riken.jp) (S. Shimoda).

problem can contribute to understanding the inner workings of the brain and to pinpointing regions with conductivity anomalies that might indicate damaged tissue (Pascual-Marqui, 1999). The EEG inverse problem is an ill-posed problem; thus, there is not a unique solution. To reconstruct an approximate solution, we need regularization techniques and methods like minimum norm estimates (MNE) (Grech et al., 2008) and low resolution electrical activity tomography (LORETA) (Grech et al., 2008; Pascual-Marqui et al., 2002, 1999). These methods consider the relationship between the current sources and the measured potentials assuming a quasi-static approximation expressed by the lead field matrix (Weinstein et al., 1999).

In this work, we propose to solve the EEG inverse problem by using the bidomain model (Sundnes, 2007). The bidomain is a reaction-diffusion model for the electrical activity of the heart and takes into account the anisotropy of the intracellular and extracellular cell domains. Compared with other methods, it does not impose a quasi-static assumption and considers an electrical model of a cell described by a series of ordinary differential equations. The bidomain model is typically used to describe the heart's electrical activity, but it was adapted as an alternative method to solve the EEG forward problem in Yin et al. (2013) and Szmurlo et al. (2007).

Starting from the standard bidomain formulation, we coupled the model to the node lead field matrix and created the necessary operators to solve the inverse problem, which gives a relationship between the scalp potentials and the stimuli in the cell model. Compared with other source localization methods, the bidomain method maintains the continuum assumption. Instead of applying regularization techniques to the current sources, we apply the regularization to the stimuli that produce the current sources. This is similar to the approach explained in detail in Lopez-Rincon et al. (2015), but adapted to the brain.

## 2. Methods

### 2.1. Mathematical background of bidomain formulation

To explain the bidomain formulation, it is necessary to give a brief overview of the lead field matrix, MNE, and LORETA methods for the EEG source localization problem.

#### 2.1.1. The lead field matrix

The EEG-measured neural activity from the brain can be described by Poisson's equation for electrical conduction (De Munck et al., 1988; Weinstein et al., 1999)

$$\nabla \cdot \sigma \nabla \Phi = -I \quad \text{in } \Omega, \quad (1)$$

with the boundary condition

$$\sigma \nabla \Phi \cdot \mathbf{n} = 0 \quad \text{on } \Gamma, \quad (2)$$

where  $\Phi$  represents the electrostatic potentials,  $\sigma$  the conductivity,  $I$  the current sources in the brain volume,  $\mathbf{n}$  the outward normal vector,  $\Gamma$  the surface area of the head, and  $\Omega$  the volume of the head. In EEG modeling, we consider the normal component of the current density to be zero as a boundary condition. Using finite element method (FEM) discretization in a 3D mesh, we can write Eqs. (1) and (2) as a system of linear equations, which may be written in matrix form (Sundnes, 2007; Gockenbach, 2006):

$$\mathbf{A}\mathbf{u} = \mathbf{I} \quad (3)$$

where

$$\mathbf{A}_{ij} = \int_{\Omega} \nabla \phi_i \cdot \nabla \phi_j,$$

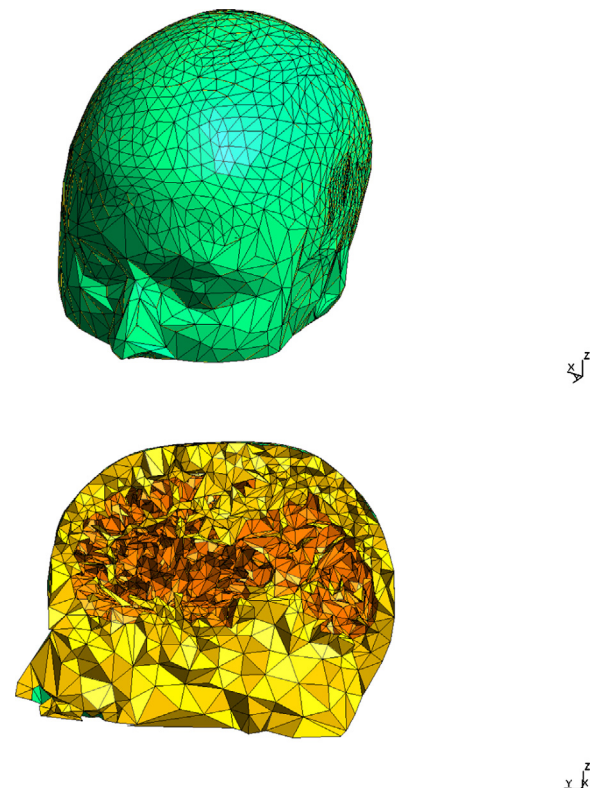


**Fig. 1.** Top: 3D mesh of a head divided into tetrahedra using FEM. In this geometry, the head is the domain  $\Omega$  and the outer surface is the domain  $\Gamma$ . Bottom: FEM discretization of the domains.

$$\mathbf{I}_i = \int_{\Omega} I \phi_i,$$

and  $\mathbf{u}$  is a vector with the scalar node values of the potential, for basis functions  $\phi_i$  and  $\phi_j$  (Fig. 1).

The model described in Eq. (1) is known as the pure Neumann problem and has no unique solutions; however, applying additional constraints—for example, reducing it to Laplace's equation (Johnson and MacLeod, 1998), fixing one electrode on the scalp to zero (Becker et al., 1982; Troparevsky and Rubio, 2003) or using the method described in Bochev and Lehoucq (2005)—gives a unique solution. From the system in Eq. (3) we can construct the lead field matrix  $\mathbf{L}$  which gives a projection between the current sources in the brain volume and the measured electrical activity in the scalp:

$$\mathbf{r} = \mathbf{L} \cdot \mathbf{s} + \text{noise}. \quad (4)$$

Here,  $\mathbf{L}$  is the lead field matrix,  $\mathbf{r}$  is a vector of the measured potentials on the head, and  $\mathbf{s}$  a vector of the current sources in the brain volume. For our tests, we use the node lead field matrix as described in Weinstein et al. (1999) and thereby reconstruct not only the current sources, but also the potential in the brain volume. The lead field matrix will typically be non-invertible as it depends on the quantity of sources and recordings. Thus, it is necessary to use regularization methods to solve the inverse problem

$$\min_{\mathbf{s}} \|\mathbf{L}\mathbf{s} - \mathbf{r}\|. \quad (5)$$

#### 2.1.2. Minimum norm estimates

The MNE (Grech et al., 2008) method is suitable for reconstructing the activity on the cortical surface. This method will give the minimum energy solution (closest to zero). MNE does not have an inclusion of priori restrictions that allow approximating a solution closer to the actual physical behavior in the brain from the set of

possible solutions (Vogel, 2002; Wang et al., 2011). Eq. (5) in terms of the brain sources is equal to

$$\mathbf{s} = [\mathbf{L}^T \mathbf{L} + \mu \mathbf{I}]^{-1} \mathbf{L}^T \mathbf{r}, \quad (6)$$

where  $\mathbf{I}$  is the identity matrix, and  $\mu$  the regularization parameter. To choose the regularization parameter we use the L-curve algorithm (Hansen and O'Leary, 1993). The L-curve is a parametric plot of  $(\log_{10}(\|\mathbf{L}^T \mathbf{L} \mathbf{s}_\mu - \mathbf{L}^T \mathbf{r}\|_2), \log_{10}(\|\mathbf{s}_\mu\|_2))$  for different values of the regularization parameter  $\mu$ . The optimal value of  $\mu$  for Tikhonov-0 regularization can be obtained from the maximum value of the curvature given by

$$\kappa(\mu) = \frac{\rho'' * \eta' - \rho' * \eta''}{((\rho')^2 + (\eta')^2)^{3/2}} \quad (7)$$

where

$$\rho = \log_{10}(\|\mathbf{L}^T \mathbf{L} \mathbf{s}_\mu - \mathbf{L}^T \mathbf{r}\|_2) \quad (8)$$

$$\eta = \log_{10}(\|\mathbf{s}_\mu\|_2) \quad (9)$$

### 2.1.3. Low resolution electrical tomography

LORETA is similar to the MNE method but, instead of using the identity matrix for the regularization, it uses the discrete Laplace operator. LORETA is suited to smoothly distributed sources as it takes into account the connectivity given by the discrete Laplacian ( $\Delta_D$ ) (Grech et al., 2008; Pascual-Marqui et al., 2002, 1999). In this case the solution is

$$\mathbf{s} = [\mathbf{L}^T \mathbf{L} + \mu \Delta_D^T \Delta_D]^{-1} \mathbf{L}^T \mathbf{r}. \quad (10)$$

### 2.1.4. Bidomain formulation for brain activity propagation

The bidomain model assumes that electrical activity is generated by the depolarization of the cell membrane between the intracellular and extracellular domains (Sundnes, 2007; Henriquez, 1992). The bidomain approach was developed to describe to electrical activity in cardiac tissue, but since then it has been adapted to other systems, such as the brain (Szmurlo et al., 2006, 2007; Yin et al., 2013). This model has the advantage of combining the overall electrical activity of the brain and the discrete nonlinear cell model. For each point in the mesh it solves the cell model and then, through diffusion, calculates the overall electrical activity of the brain. The bidomain model is described by the following equations (Tung, 1978):

$$\nabla \cdot (M_i \nabla v) + \nabla \cdot (M_i \nabla u_e) = \beta(C_m \frac{\partial v}{\partial t} + I_{ion}(v, w) + I_{app}), \quad (11)$$

$$\nabla \cdot (M_i \nabla v) = -\nabla \cdot ((M_i + M_e) \nabla u_e), \quad (12)$$

where  $v$  is the transmembrane potential,  $u_e$  is the extracellular potential,  $M_i$  is the intracellular conductivity tensor,  $M_e$  is the extracellular conductivity tensor,  $C_m$  is transmembrane capacitance, and  $\beta$  is the membrane surface to volume ratio. If we assume a linear relationship between the intra- and extracellular conductivity tensor,  $M_e = \lambda M_i$ , where  $\lambda$  is a constant scalar, we can reduce the bidomain model to a monodomain model:

$$\frac{\lambda}{1 + \lambda} \nabla \cdot (M_i \nabla v) = \beta(C_m \frac{\partial v}{\partial t} + I_{ion}(v, w) + I_{app}), \quad (13)$$

with the boundary condition

$$(M_i \nabla v) \cdot \mathbf{n} = 0, \quad (14)$$

and the following equation to get the extracellular potential

$$\nabla \cdot (M_i \nabla v) = -\nabla \cdot ((1 + \lambda) M_i \nabla u_e). \quad (15)$$

We will scale the equations with

$$M_i = \frac{M_i}{C_m \beta}. \quad (16)$$

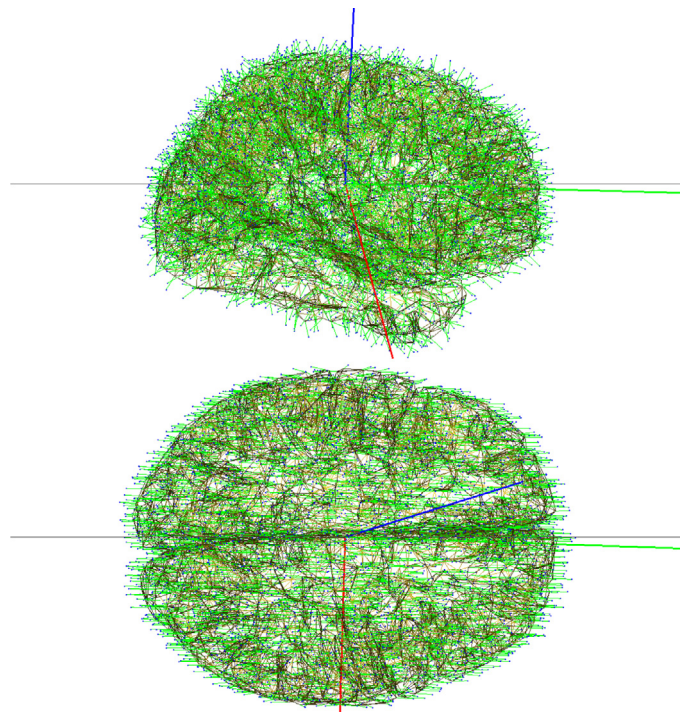


Fig. 2. Lateral and superior views of the brain mesh showing the fiber directions.

to simplify the notation. The bidomain and monodomain models are dependent on the fiber direction for approximating the propagation of electrical activity. To create the fiber directions, we use the white matter in the brain mesh and draw the fiber directions tangent to the surface taking into account the anisotropy in white matter (the anisotropy in gray matter is negligible) (Hallez et al., 2007b) giving the fiber directions represented in Fig. 2.

### 2.1.5. The monodomain inverse operator

From Eq. (13) we create the operators to solve the inverse problem using a method similar to that explained in detail in (Lopez-Rincon et al., 2015). To solve the monodomain model numerically, we use the Godunov operator splitting technique (Sundnes, 2007) to divide the system into an ionic part (Eq. (17)) and a diffusion part (Eq. (18)):

$$\frac{\partial v}{\partial t} = -I_{ion}(v, w) - I_{app}, \quad (17)$$

$$\frac{\partial v}{\partial t} = \frac{\lambda}{1 + \lambda} \nabla \cdot (M_i \nabla v). \quad (18)$$

Then, we first solve

$$\frac{\partial sp_1}{\partial t} = -I_{ion}(v, w) - I_{app}, \quad (19)$$

$$sp_1(0) = v(0) \quad (20)$$

for  $t \in [0, \Delta t]$ . This gives us  $sp_1(\Delta t)$ . Next, we solve

$$\frac{\partial sp_2}{\partial t} = \frac{\lambda}{1 + \lambda} \nabla \cdot (M_i \nabla sp_2), \quad (21)$$

$$sp_2(0) = sp_1(\Delta t) \quad (22)$$

for  $t \in [0, \Delta t]$  to get  $sp_2(\Delta t)$  which we set equal to

$$v(\Delta t) = sp_2(\Delta t). \quad (23)$$

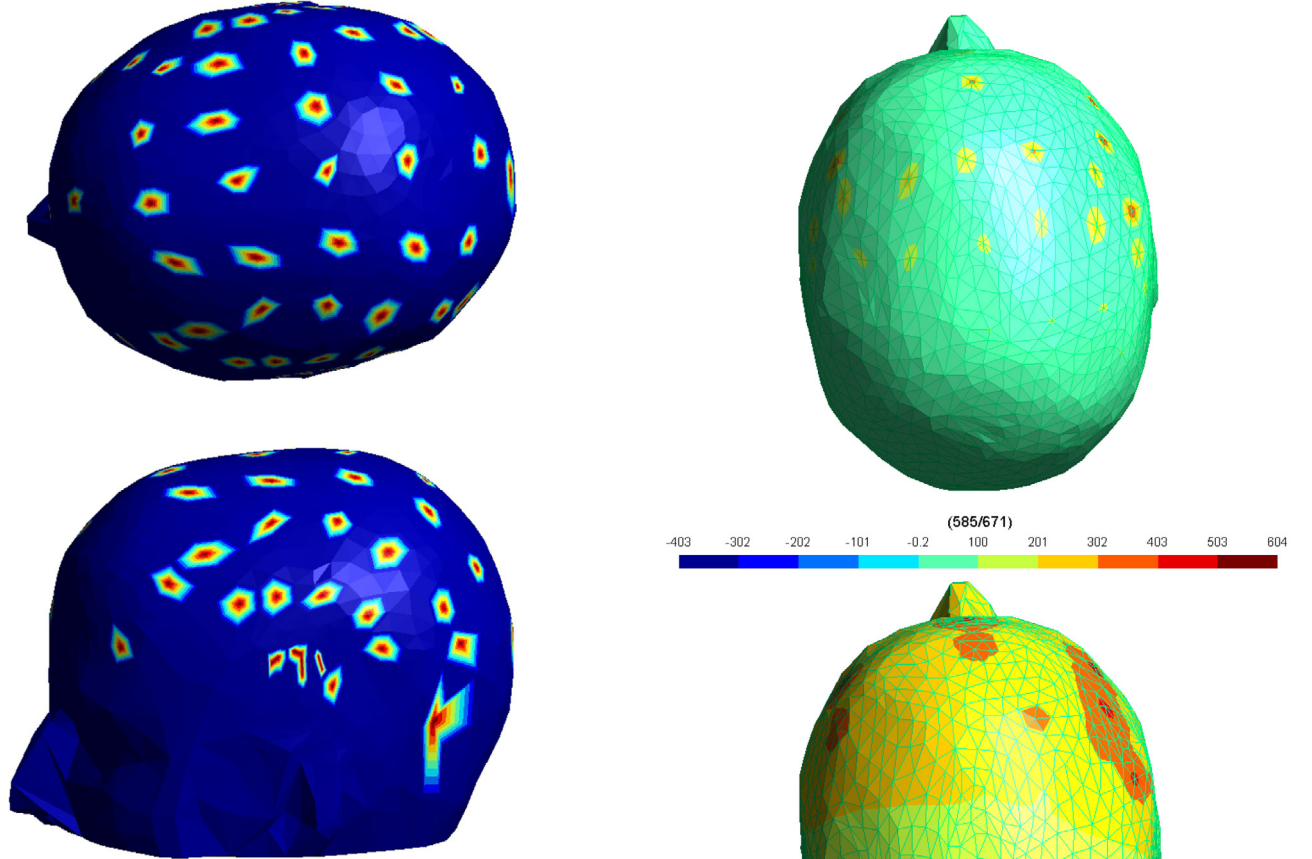


**Fig. 3.** Superior and lateral views of the EEG electrode positions.

Thus, we can solve the system in steps. If we discretize Eq. (17) over time, we obtain

$$\frac{v_{n+1} - v_n}{\Delta t} = -I_{ion}(v_n, w_n) - I_{app}, \quad (24)$$

or

$$v_{n+1} = -\Delta t I_{ion}(v_n, w_n) - \Delta t I_{app} + v_n. \quad (25)$$

Eq. (18) is discretized using the  $\theta$  rule:

$$\frac{v_{n+2} - v_{n+1}}{\Delta t} = \theta \left( \frac{\lambda}{1 + \lambda} \nabla \cdot (M_i \nabla v_{n+2}) \right) + \left( (1 - \theta) \frac{\lambda}{1 + \lambda} \nabla \cdot (M_i \nabla v_{n+1}) \right). \quad (26)$$

Multiplying by a test function  $\psi$  and rearranging the terms, we have

$$\begin{aligned} v_{n+2} \psi - \theta \left( \frac{\Delta t \lambda}{1 + \lambda} \nabla \cdot (M_i \nabla v_{n+2}) \right) \psi \\ = v_{n+1} \psi + \left( (1 - \theta) \frac{\Delta t \lambda}{1 + \lambda} \nabla \cdot (M_i \nabla v_{n+1}) \right) \psi. \end{aligned} \quad (27)$$

Applying Green's identity to Eq. (27) gives

$$\begin{aligned} \int_{\Omega_H} v_{n+2} \psi + \theta \left( \frac{\Delta t \lambda}{1 + \lambda} \right) \int_{\Omega} M_i \nabla v_{n+2} \nabla \psi - \int_{\partial\Omega} M_i \psi \nabla v_{n+2} \cdot \mathbf{n} \\ = \int_{\Omega_H} v_{n+1} \psi - (1 - \theta) \frac{\Delta t \lambda}{1 + \lambda} \int_{\Omega} M_i \nabla v_{n+1} \nabla \psi \\ + \int_{\partial\Omega} M_i \psi \nabla v_{n+1} \cdot \mathbf{n}. \end{aligned} \quad (28)$$

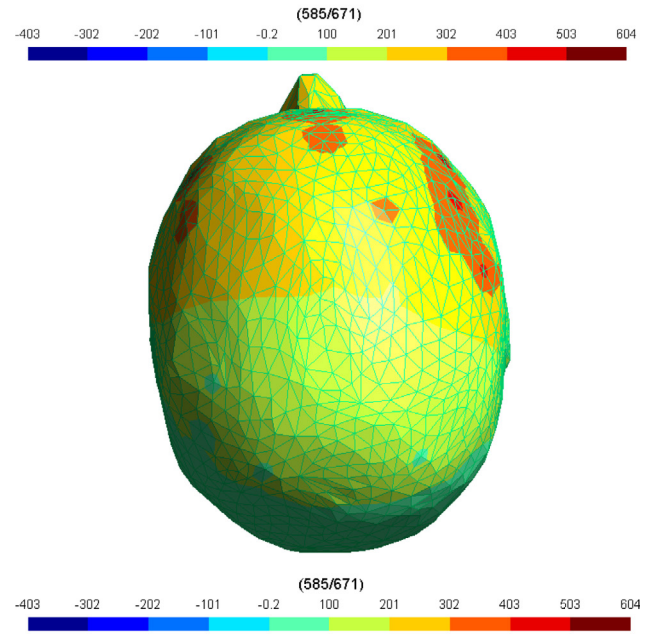


**Fig. 4.** BEM Laplace interpolation of electrode values.

We will consider  $v_{n+1}$  and  $v_{n+2}$  as linear combinations of basis functions:

$$v_{n+1} = \sum_{j=1}^N v_j^{n+1} \phi_j, \quad (29)$$

$$v_{n+2} = \sum_{j=1}^N v_j^{n+2} \phi_j \quad (30)$$

where  $N$  is the number of nodes in the brain volume. Thus, by applying the FEM approximation, Eq. (28) becomes

$$\begin{aligned} \sum_{j=1}^N v_j^{n+2} \left( \int_{\Omega} \phi_j \phi_i + \theta \left( \frac{\Delta t \lambda}{1 + \lambda} \right) \int_{\Omega} M_i \nabla \phi_j \nabla \phi_i \right) \\ = \sum_{j=1}^N v_j^{n+1} \left( \int_{\Omega} \phi_j \phi_i - (1 - \theta) \frac{\Delta t \lambda}{1 + \lambda} \int_{\Omega} M_i \nabla \phi_j \nabla \phi_i \right), \quad i, j = 1, \dots, N \end{aligned} \quad (31)$$

and we get the following matrices.

$$\mathbf{A}_{ij} = \int_{\Omega} \phi_j \phi_i + \theta \left( \frac{\Delta t \lambda}{1 + \lambda} \right) \int_{\Omega} M_i \nabla \phi_j \nabla \phi_i, \quad (32)$$

$$\mathbf{B}_{ij} = \int_{\Omega} \phi_j \phi_i - (1 - \theta) \frac{\Delta t \lambda}{1 + \lambda} \int_{\Omega} M_i \nabla \phi_j \nabla \phi_i. \quad (33)$$

>From Eqs. (32) and (33), we can construct the matrix equation

$$\mathbf{AV}_{n+2} = \mathbf{BV}_{n+1}, \quad (34)$$

where  $\mathbf{V}_{n+2}$  and  $\mathbf{V}_{n+1}$  are the vectors with the nodal values for iterations  $n+1$  and  $n+2$  in the numerical solution. From Eq. (15) we derive a relationship between the transmembrane potential and the extracellular potential, given by

$$\mathbf{RV}_{n+2} = \mathbf{QU}_e. \quad (35)$$

From Eqs. (34) and (35) we can explicitly construct a vector with the nodal values for the extracellular potential  $\mathbf{U}_e$  as

$$\mathbf{U}_e = \mathbf{Q}^{-1} \mathbf{RA}^{-1} \mathbf{BV}_{n+1}. \quad (36)$$

A relationship with the voltage distribution over the scalp can be constructed using the lead field matrix  $\mathbf{L}$  multiplied by a Dirichlet-to-Neumann operator ( $\mathbf{A}_{bb}^{-1}$ ) to transform currents in the brain volume into potentials  $\mathbf{T} = \mathbf{LA}_{bb}^{-1}$ .

$$\mathbf{TQ}^{-1} \mathbf{RA}^{-1} \mathbf{BV}_{n+1} = \mathbf{r}, \quad (37)$$

or

$$\mathbf{TQ}^{-1} \mathbf{RA}^{-1} \mathbf{B}(-\Delta t \mathbf{I}_{ion} - \Delta t \mathbf{I}_{app} + \mathbf{V}_n) = \mathbf{r}, \quad (38)$$

where  $\mathbf{I}_{app}$  and  $\mathbf{I}_{ion}$  are vectors with the nodal values for the applied current and ionic flux. From this we will create the operator

$$\mathbf{P} = \mathbf{TQ}^{-1} \mathbf{RA}^{-1} \mathbf{B}, \quad (39)$$

and

$$-\mathbf{P} \Delta t \mathbf{I}_{ion} - \mathbf{P} \Delta t \mathbf{I}_{app} + \mathbf{PV}_n = \mathbf{r}. \quad (40)$$

The EEG inverse problem is an ill-posed problem, making a regularization technique necessary. We used the following Tikhonov functional:

$$\min_{\mathbf{I}_{app}} (\| -\mathbf{P} \Delta t \mathbf{I}_{app} - \mathbf{r} - \mathbf{P} \Delta t \mathbf{I}_{ion} \|^2 + \mu \| \mathbf{C}(\mathbf{I}_{app} - \mathbf{I}_{app}') \|^2), \quad \mu > 0, \quad (41)$$

or

$$\min_{\mathbf{s}} (\| -\mathbf{P} \Delta t \mathbf{s} - \mathbf{r} - \mathbf{P} \Delta t \mathbf{I}_{ion} \|^2 + \mu \| \mathbf{C}(\mathbf{s} - \mathbf{s}') \|^2), \quad \mu > 0, \quad (42)$$

with the L-Curve method (Hansen and O'Leary, 1993) to find the regularization parameter. Here  $\mathbf{C}$  is a constrained matrix (the identity matrix), and  $\mathbf{s}'$  is the prior information ( $\mathbf{s}' = 0$ ). For our tests, we use  $\mu = 0.05$ .

### 2.1.6. Error estimation

The error is given by the difference between the original potential distribution and the solution obtained by each method, as in Lopez-Rincon et al. (2015):

$$error = \sum_i^N \sum_j^{\text{Nodes}} |\mathbf{U}_{e(\text{original})}^{i,j} - \mathbf{U}_{e(\text{calculated})}^{i,j}| \quad (43)$$

where  $\mathbf{U}_{e(\cdot)}^{i,j}$  are the nodal values of the potential for the original and reconstructed distributions,  $\text{Nodes}$  is the maximum number of nodes, and  $N$  is the total number of samples.

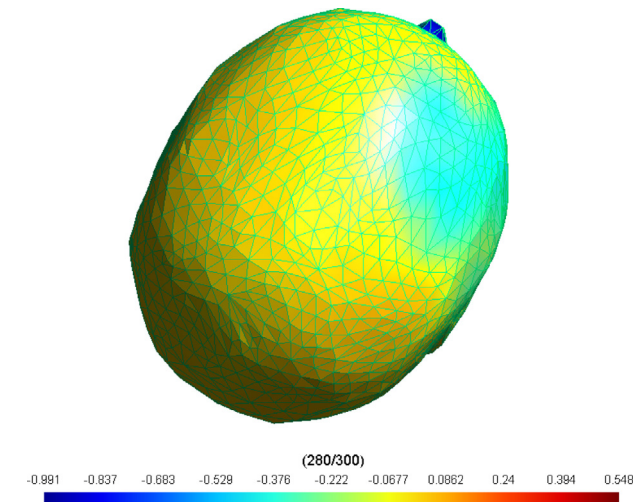


Fig. 5. Simulated spike values on the head.

## 2.2. Implementation

For the implementation, we created several modules using the described methods in the C# programming language. For the example of real data, we implemented an EDF reader for the Physionet Physiobank database (Schalk et al., 2004; Goldberger et al., 2000). We created a module in OpenGL to visualize and modify 3D meshes to create the fiber directions for the method and visualize the electrical activity. The mesh used in all the examples consists of 35,982 elements. For the visualization of the results we added a plug-in to output the results in Gmsh format (Geuzaine and Remacle, 2009) (Fig. 3).

### 2.2.1. Data preprocessing

To use the EEG signals we need to preprocess the data. The first step is to allocate the electrode signals to a node in the head mesh. The EEG signals were recorded from 64 electrodes following the international 10-10 system (Schalk et al., 2004). Then, for each sample in the dataset, with  $N$  being the total number of samples we solve the Laplace equation using the boundary element method (BEM) (Schlitt et al., 1995; Nintcheu Fata, 2009) with the following conditions: each given electrode position will be considered a Dirichlet boundary condition, and the rest will be considered a null-flux Neumann condition. The result is shown in Fig. 4. Then, we make a second interpolation in time to match the time step to be used in the bidomain formulation ( $\Delta t$ ). Finally, we normalize the data. This procedure is summarized in Algorithm 1.

#### Algorithm 1. Preprocessing of the data

---

**Input:** Head mesh, EEG signals  
**Output:** Interpolated, normalized signals on the scalp

- 1 Position the signals in the scalp mesh as in the 10-10 system;
- 2 **for** each sample in  $N$  **do**
  - Perform Laplace interpolation using BEM;
- 3 Perform time interpolation to match  $\Delta t$  from the bidomain;
- 4 Normalize the signals;

---

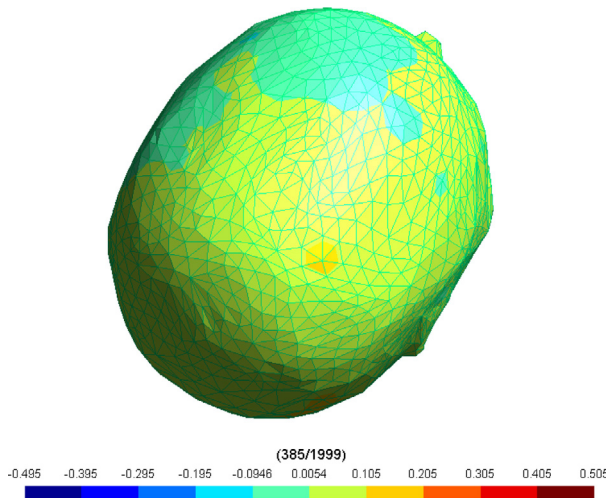


**Fig. 6.** Measured spike values on the head from a real EEG measurement.

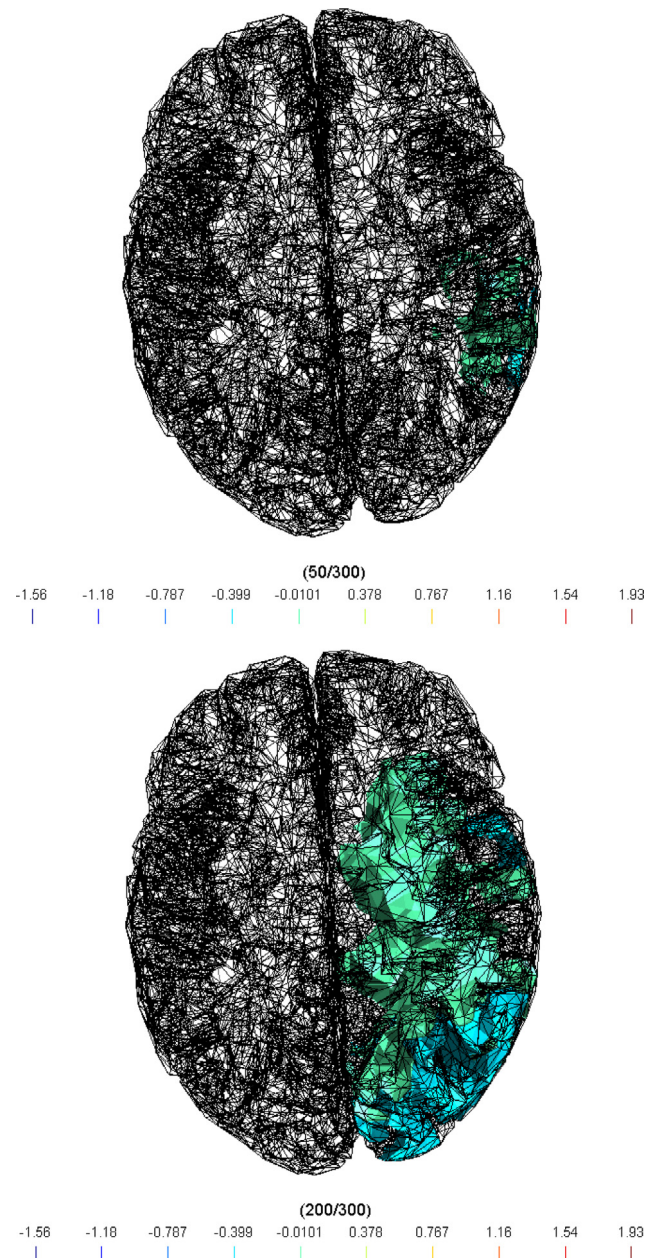


**Fig. 7.** Original distributions for the forward problem with one source at 50 ms and 200 ms.

### 3.1. Comparison of the MNE, LORETA, and bidomain methods for one source

We put one source in the brain volume and construct the potentials in the scalp. Then, we solved the inverse problem with MNE (Fig. 8), LORETA (Fig. 9) and the bidomain approach (Fig. 10). In each case, we compare the solution to the original distributions (Fig. 7) at 50 ms and 200 ms.

### 3.2. Comparison of the MNE, LORETA, and bidomain methods for three sources

We put three sources in the brain volume and constructed the potentials in the scalp. Then, we solved the inverse problem with MNE (Fig. 12), LORETA (Fig. 13) and the bidomain approach (Fig. 14). In each case, we compared the solution to the original distribution (Fig. 11).

## 3. Results

### 3.0.1. Example of the forward problem

Using the procedure for the bidomain model described in Szmurlo et al. (2006), we created electrical activity in the scalp. The EEG simulated data are shown in Fig. 5, and the measured scalp values from the EEG Motor Movement/Imagery Dataset of the Physiobank are shown in Fig. 6 (Schalk et al., 2004; Goldberger et al., 2000).

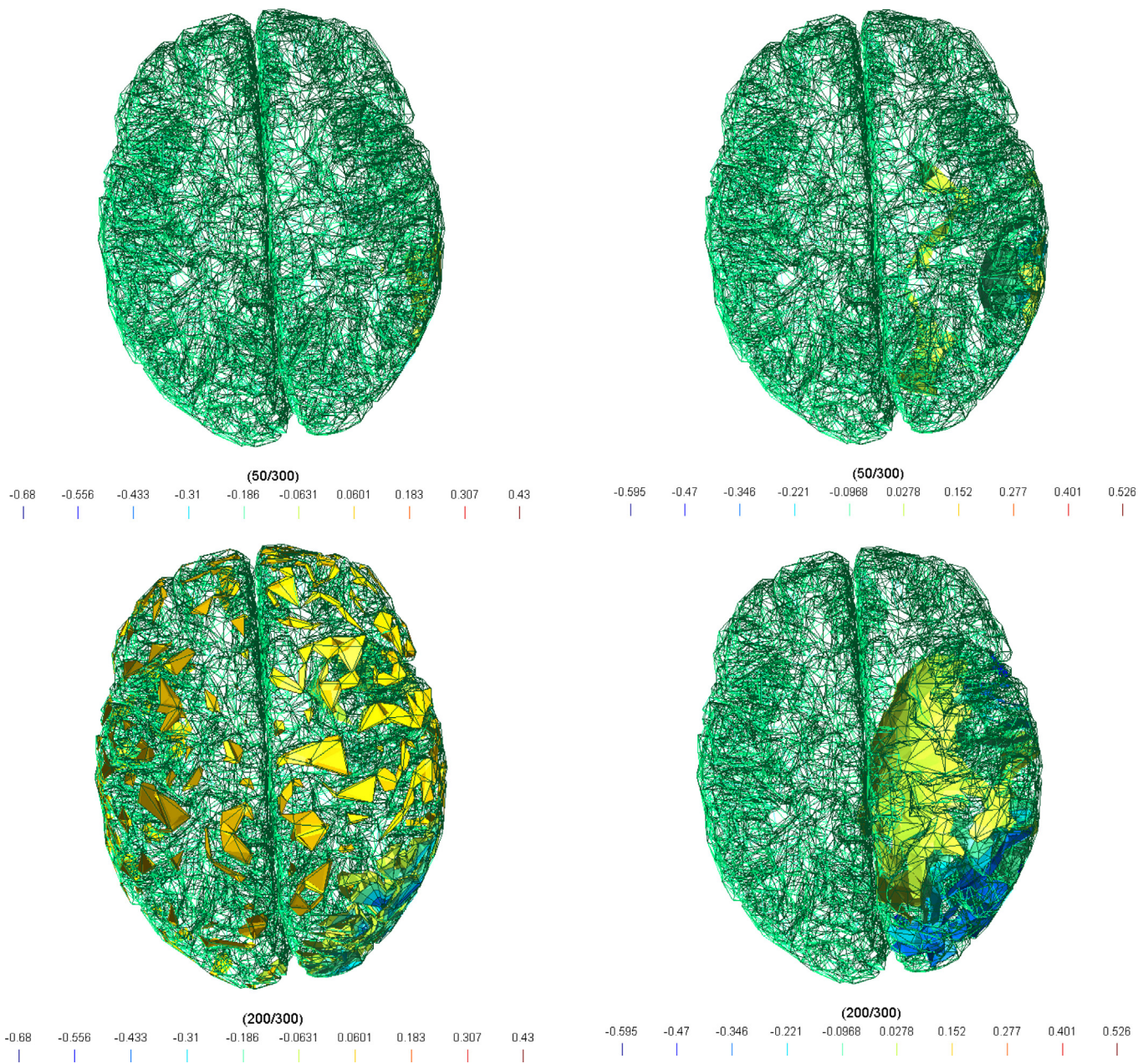


**Fig. 8.** MNE solution for one source at 50 ms and 200 ms.

**Fig. 9.** LORETA solution for one source at 50 ms and 200 ms.

**Table 1**  
Comparison of errors for each test.

|               | MNE    | LORETA | Bidomain |
|---------------|--------|--------|----------|
| One source    | 11.2e4 | 41.4e3 | 31.1e3   |
| Three sources | 16.9e4 | 67.4e3 | 65.4e3   |

To make a comparison, we calculate the error given by Eq. (43) for each method. These errors are summarized in [Table 1](#).

### 3.2.1. Time comparison

We next compare the different methods using a computer with an Intel(R) Core(TM) i7-2860QM CPU @ 2.50Hz and 8.00 Gb RAM. The times in ms for reconstruction programmed using C# and OpenGL for the graphics are shown in [Table 2](#).

This time is dependent of the processor in the computer; therefore, the values here should be taken as giving only an overall idea.

**Table 2**  
Comparison of reconstruction times in ms for each test.

|                   | One point | Three points |
|-------------------|-----------|--------------|
| MNE               | 7110906   | 7111203      |
| LORETA            | 10308247  | 10311428     |
| Bidomain operator | 13510721  | 13511285     |

### 3.3. Response to visual stimuli

The EEG Motor Movement/Imagery Dataset ([Schalk et al., 2004](#)) from the Physiobank ([Goldberger et al., 2000](#)) has a series of measurements for different tasks. We used the recordings where a visual stimulus appears on a screen and then the subject closes his/her fist. The measurements originated from recordings made with a 64-channel EEG system (BCI2000).

Using the bidomain formulation, we solved the EEG inverse problem to reconstruct the response to visual stimuli in the brain

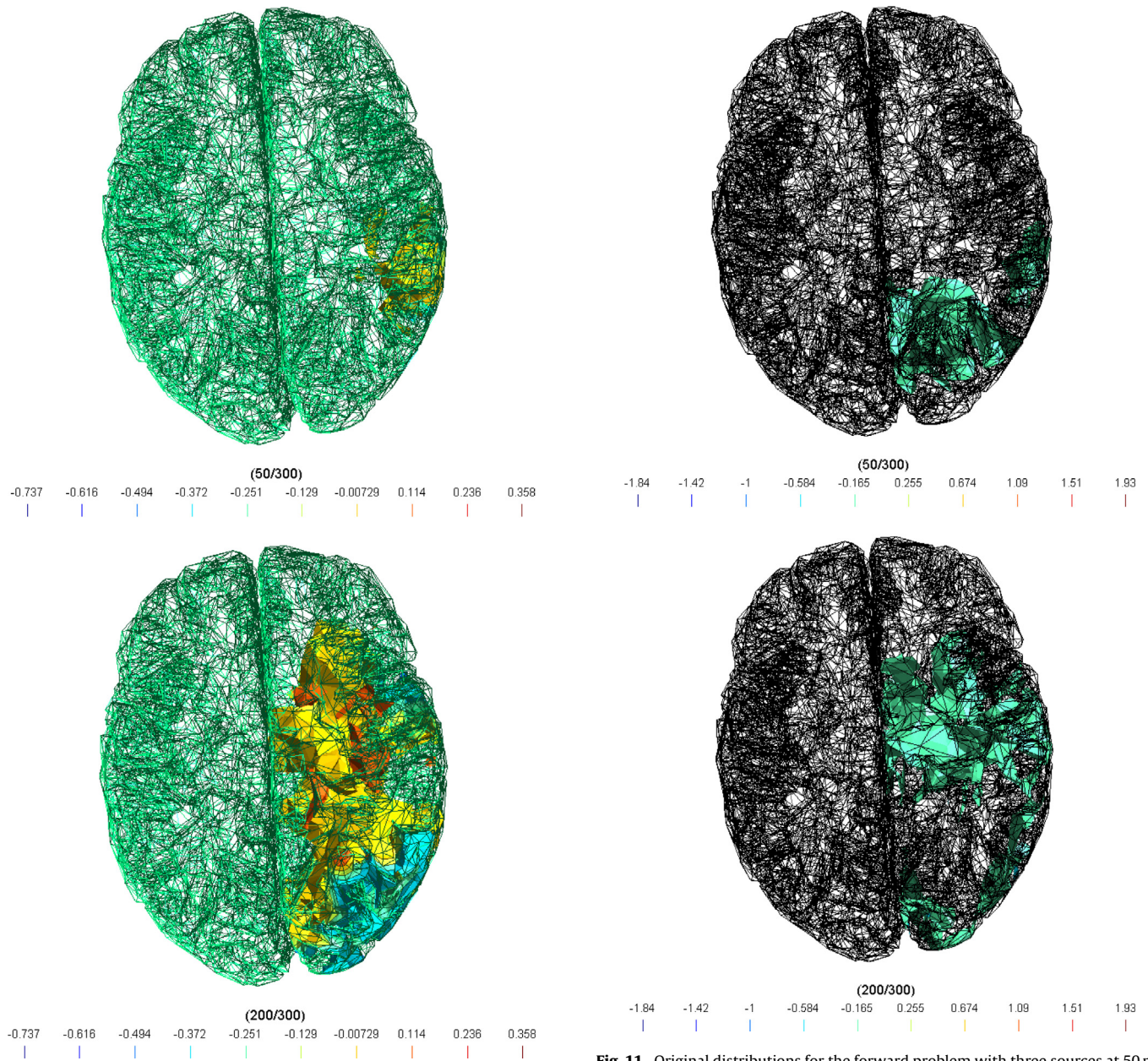


**Fig. 10.** Bidomain solution for one source at 50 ms and 200 ms.

**Fig. 11.** Original distributions for the forward problem with three sources at 50 ms and 200 ms.

volume. From the different subjects, we obtained the timings between the stimulus being received in the brain and the reaction to it. The exact time depends on the subject, but on average remains the same. In Fig. 15, the addition of the absolute value of the electrical activity in the brain (vertical axis) is shown for two subjects in two different tasks for half a second (horizontal axis).

Measuring the time between the centers of the first and second highest peaks for 45 reconstructions gives an average of 0.246666667 s, which is consistent with the timing of the visual stimulus being detected in the observer's brain before he/she manually responds to the stimulus (Amano et al., 2006).

Comparing the position of the second spike shown Fig. 17 with data from the platform LinkRbrain, which is a collection of data that shows the greatest activity in the fMRI bold signal during several tasks, we find that the results are consistent with hand movement (Fig. 16).

#### 4. Discussion

First we simulated a spike in the brain using the forward bidomain method, as given in (Szmurlo et al., 2006; Yin et al., 2013), to show that the system works.

Then we made a comparison of the MNE, LORETA, and bidomain approaches to the inverse problem using synthetic data for one and three cortical sources. We chose to compare our approach with MNE because it is a method suited for reconstructing sources on the cortical surface with and LORETA because it gives satisfactory results in EEG source analysis (Grech et al., 2008). From a comparison of the original distribution with the ones created with the cost functional in Eq. (41) and with the ones from MNE and the LORETA model, by visual inspection of the relevant images, it is clear that using the dynamic model gives more precise results.

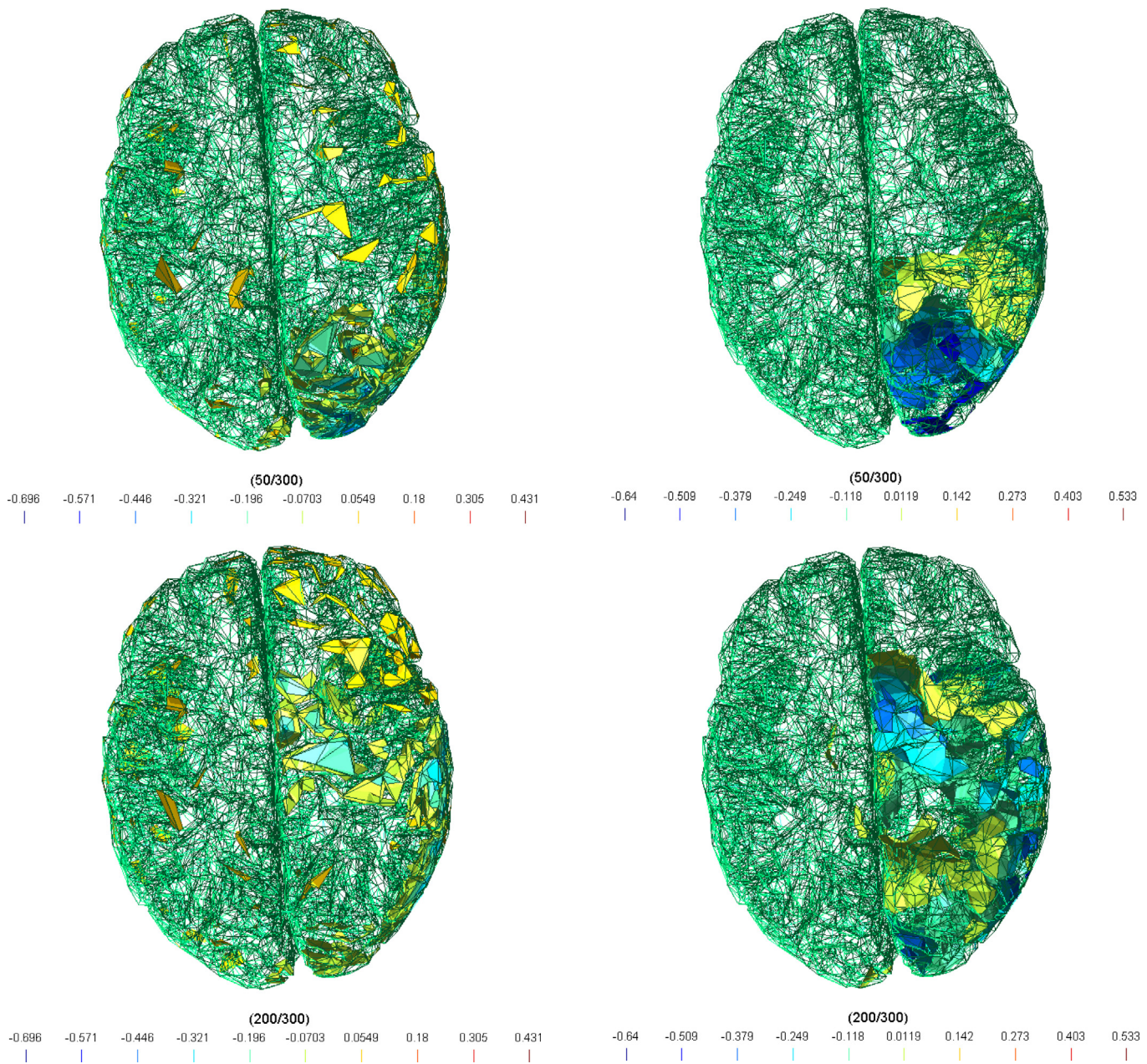


**Fig. 12.** MNE solution for three sources at 50 ms and 200 ms.

As is well known, EEG source localization is an ill-posed problem. Our approach attacked this problem by modeling a EEG dynamic changes computing from a dynamics of neuron activities. The observations of EEG dynamic changes can change EEG source localization problem to a well-posed problem. This is a remarkable point of our approach that distinguish our method from the conventional approaches with the quasi-static models and possible to provide more precise results as mentioned above.

We used real measurement data and calculated the inverse solution for three subjects undertaking 15 tasks each, to estimate the time delay between the first two highest activity peaks. We reconstructed the electrical activity in the brain for the Physiobank EEG Motor Movement/Imagery Dataset and used measurements from 64 electrodes on the scalp for the fist-closing action (Schalk et al., 2004; Goldberger et al., 2000). When these data were collected, the subjects received a visual stimulus and then closed their fists. In the reconstructed activity, the first spike is considered as brain activity

generated from the visual stimulus and the second as the response to it.

To validate our results, we compared the spatial representation of the highest activity with LinkRbrain (Mesmoudi et al., 2015). LinkRbrain is an open-access web platform for multi-scale data integration and visualization. The functional part of this tool (300 sensorimotor/cognitive functions) was reconstructed from the fMRI literature (5000 papers). For our experiments, we choose the hand movement task in the database as a reference and compared the highest activity peaks with the reconstructed inverse solution from the bidomain formulation. The positions of the peaks are consistent with those in the database. Finally, we compared the time delay between the reception of the visual stimulus and the intention of movement for the hand movement task. The time delays are consistent with what is found in literature for the visual stimulus response and hand movement task.

**Fig. 13.** LORETA solution for three sources at 50 ms and 200 ms.

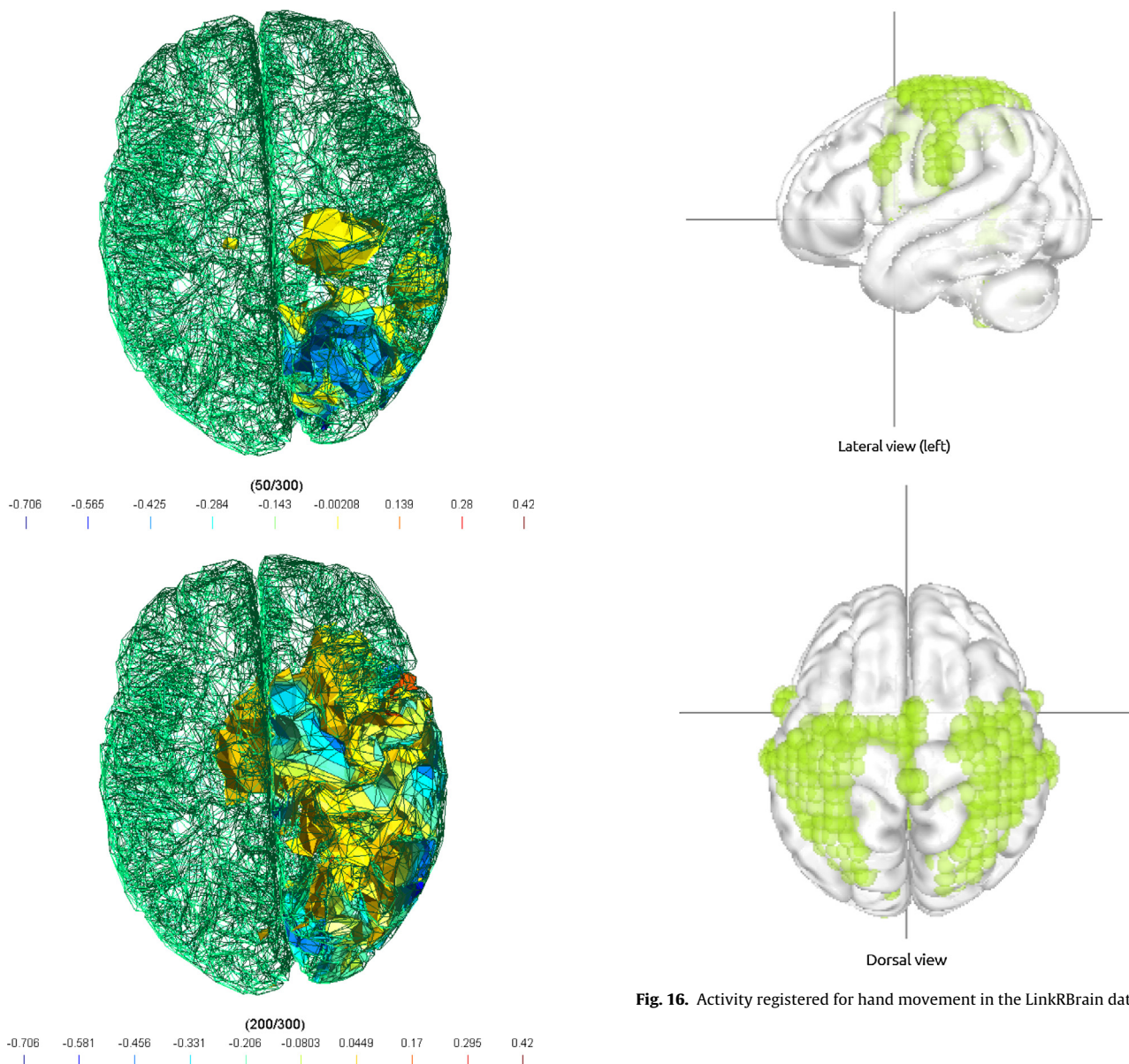


**Fig. 14.** Bidomain solution for three sources at 50 ms and 200 ms.

**Fig. 16.** Activity registered for hand movement in the LinkRBrain database.

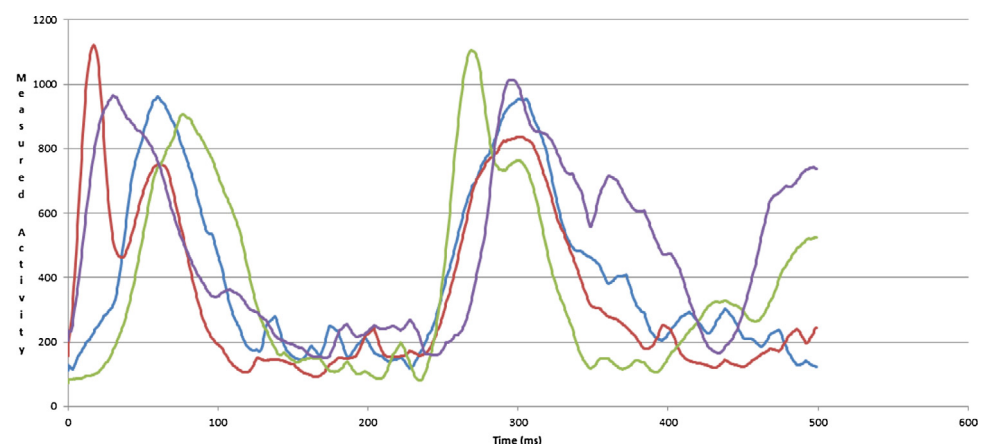


**Fig. 15.** Overall activity in the brain from 2 subjects for hand movement.

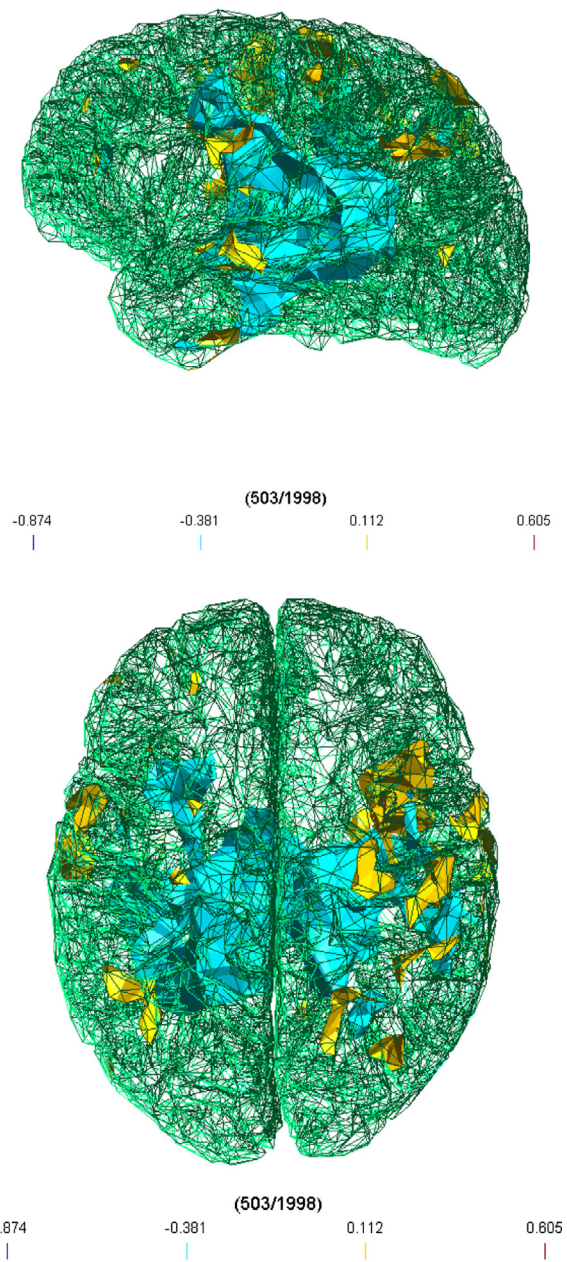


**Fig. 17.** Activity reconstructed by solving the bidomain inverse problem.

## 5. Conclusion

In this paper, we applied the bidomain formulation to the inverse problem of brain activity source localization from EEG signals. The inverse bidomain formulation allows us to take into account the non-linearity of the cell models, time propagation, and the anisotropy in the conductivity of the brain volume tissue, in comparison to other methods.

The method makes a construction of the sources considering the dynamic natural depolarization and not the quasi-static approach as other methods (Baillet et al., 2001; Gener and Williamson, 1998; Pascual-Marqui, 1999). In other words, the proposed method uses the solution at time  $n$  to construct the solution at time  $n+1$ , not only the EEG signals at time  $n+1$ . The results show that this method gives a better reconstruction for source localization in comparison with the quasi-static approach.

In an example of visual stimulus and response, the reconstruction appears to be temporally and spatially close to reality.

However, it should be remembered that we are working with archived measurements and not readings from the original brain and head mesh of subjects. With the necessary pre-processing and a powerful enough computer, this method could be performed in real time, as can be done with MNE or LORETA. In future work, we will divide the EEG measurements into different frequency bands to see if we are able to classify movement intention from the inverse solution.

## Acknowledgments

This work was conducted as part of a collaboration between the RIKEN Brain Research Institute and Toyota Motor Company.

## References

- Amano, Kaoru, et al., 2006. Estimation of the timing of human visual perception from magnetoencephalography. *J. Neurosci.* 26 (15), 3981–3991.
- Baillet, S., et al., 2001. Evaluation of inverse methods and head models for EEG source localization using a human skull phantom. *Phys. Med. Biol.* 46 (1), 77.
- Becker, E.B., et al., 1982. Finite elements, an introduction. *J. Appl. Mech.* 49, 682.
- Bochev, Pavel, Lehoucq, Richard B., 2005. On the finite element solution of the pure Neumann problem. *SIAM Rev.* 47 (1), 50–66.
- Brannon, Elizabeth M., et al., 2008. *Principles of Cognitive Neuroscience*. Vol. 83. Sinauer Associates, Sunderland, MA.
- De Munck, Jan C., Van Dijk, Bob W., Spekreijse, Henk, 1988. Mathematical dipoles are adequate to describe realistic generators of human brain activity. *Biomed. Eng., IEEE Transactions on* 5 (11), 960–966.
- Gener, Nevezat G., Williamson, Samuel J., 1998. Differential characterization of neural sources with the bimodal truncated SVD pseudo-inverse for EEG and MEG measurements. *IEEE Trans. Biomed. Eng.* 45 (7), 827–838.
- Geuzaine, Christophe, Remacle, Jean-François, 2009. Gmsh: A 3-D finite element mesh generator with built-in pre-and post-processing facilities. *Int. J. Numer. Methods Eng.* 79 (11), 1309–1331.
- Gockenbach, Mark S., 2006. *Understanding and Implementing the Finite Element Method*. Siam.
- Goldberger, A.L., Amaral, L.A.N., Glass, L., Hausdorff, J.M., Ivanov, P.Ch., Mark, R.G., Mietus, J.E., Moody, G.B., Peng, C.-K., Stanley, H.E., 2000 June 13. PhysioBank, PhysioToolkit, and PhysioNet: Components of a New Research Resource for Complex Physiologic Signals. *Circulation* 101 (23), e215–e220 [Circulation Electronic Pages; <http://circ.ahajournals.org/cgi/content/full/101/23/e215>].
- Grech, Roberta, et al., 2008. Review on solving the inverse problem in EEG source analysis. *J. Neuroeng. Rehabil.* 5 (1), 1.
- Hallez, Hans, et al., 2007a. Review on solving the forward problem in EEG source analysis. *J. Neuroeng. Rehabil.* 4 (1), 1.
- Hallez, Hans, et al., 2007b. Importance of including anisotropic conductivities of grey matter in EEG source localization. In: 6th International Conference on Bioelectromagnetism (ICBEM2007). Vol. 9. No. 2.
- Hansen, Per Christian, O'Leary, Dianne Prost, 1993. The use of the L-curve in the regularization of discrete ill-posed problems. *SIAM J. Sci. Comput.* 14 (6), 1487–1503.
- Henriquez, Craig S., 1992. Simulating the electrical behavior of cardiac tissue using the bidomain model. *Crit. Rev. Biomed. Eng.* 21 (1), 1–77.
- Johnson, Christopher R., MacLeod, Robert S., 1998. Adaptive local regularization methods for the inverse ECG problem. *Progr. Biophys. Mol. Biol.* 69 (2), 405–423.
- Lopez-Rincon, Alejandro, Bendahmane, Mostafa, Ainseba, BedrEddine, 2015. On 3D numerical inverse problems for the bidomain model in electrocardiology. *Comput. Math. Appl.* 69 (4), 255–274.
- Mesmoudi, Salma, et al., 2015. LinkRbrain: Multi-scale data integrator of the brain. *J. Neurosci. Methods* 241, 44–52.
- Nintcheu Fata, Sylvain, 2009. Explicit expressions for 3D boundary integrals in potential theory. *Int. J. Numer. Methods Eng.* 78 (1), 32–47.
- Pascual-Marqui, Roberto D., et al., 2002. Functional imaging with low-resolution brain electromagnetic tomography (LORETA): a review. *Methods Findings Exp. Clin. Pharmacol.* 24 (Suppl C), 91–95.
- Pascual-Marqui, Roberto D., et al., 1999. Low resolution brain electromagnetic tomography (LORETA) functional imaging in acute, neuroleptic-naïve, first-episode, productive schizophrenia. *Psychiatry Res.: Neuroimaging* 90 (3), 169–179.
- Pascual-Marqui, Roberto D., 1999. Review of methods for solving the EEG inverse problem. *Int. J. Bioelectromagnetism* 1 (1), 75–86.
- Schalk, G., McFarland, D.J., Hinterberger, T., Birbaumer, N., Wolpaw, J.R., 2004. BCI2000: A General-Purpose Brain-Computer Interface (BCI) System. *IEEE Trans. Biomed. Eng.* 51 (6), 1034–1043 [In 2008, this paper received the Best Paper Award from IEEE TBME.].
- Schlitt, Heidi A., et al., 1995. Evaluation of boundary element methods for the EEG forward problem: effect of linear interpolation. *Biomed. Eng. IEEE Transactions on* 2 (1), 52–58.
- Sundnes, Joakim, et al., 2007. *Computing the Electrical Activity in the Heart*. Vol. 1. Springer Science & Business Media.

- Szmurlo, R., et al., 2006. Bidomain formulation for modeling brain activity propagation. In: Electromagnetic Field Computation, 2006 12th Biennial IEEE Conference on. IEEE.
- Szmurlo, R., et al., 2007. Multiscale finite element model of the electrically active neural tissue. EUROCON, 2007. In: The International Conference on &# 34; Computer as a Tool &# 34;; IEEE.
- Troparevsky, M.I., Rubio, D., 2003. On the weak solutions of the forward problem in EEG. *J. Appl. Math.* 2003 (12), 647–656.
- Tung, Leslie, 1978. A bi-domain model for describing ischemic myocardial dc potentials. Diss. Massachusetts Institute of Technology.
- Vogel, Curtis R., 2002. *Computational Methods for Inverse Problems*. Vol. 23. Siam.
- Wang, Yanfei, Yagola, Anatoly G., Yang, Changchun, 2011. *Optimization and Regularization for Computational Inverse Problems and Applications*. Higher Education Press, Beijing.
- Weinstein, David, Zhukov, Leonid, Johnson, Chris, 1999. Lead field basis for fem source localization. In: *Frontiers in Simulation, Simulationstechnique 18th Symposium*.
- Yin, S., Dokos, S., Lovell, N.H., 2013. Bidomain Modeling of Neural Tissue. *Neural Engineering*. Springer US, 389–404.